Journal of Gastroenterology and Hepatology

JGHF

doi:10.1111/j.1440-1746.2011.06864.x

HEPATOLOGY

Transition from hepatic steatosis to steatohepatitis: Unique microRNA patterns and potential downstream functions and pathways

Xi Jin,* Yi-peng Chen,*[1] Mei Kong,[†] Lin Zheng,[‡] Yi-da Yang[‡] and You-ming Li*

Departments of *Gastroenterology, [†]Pathology and [‡]Infectious Disease, The First Affiliated Hospital, College of Medicine, Zhejiang University, Hangzhou, Zhejiang, China

Key words
gene ontology, microarray, microRNA, non-alcoholic steatohepatitis, steatosis.

Accepted for publication 12 July 2011.

Correspondence
You-ming Li, Digestive Department, The First Affiliated Hospital, College of Medicine, Zhejiang University, No.79 Qingchun Road, Hangzhou, Zhejiang 310003, China. Email: jxfl007@hotmail.com

[1]This author contributes equally to this paper as the first author.

There exist no conflicts of interest. The founders had no role in study design, data collection and analysis, decision to publish, or preparation of the manuscript.

Abstract

Background and Aim: This study aimed to explore the unique miRNA responsible for transition from hepatic steatosis to steatohepatitis and to investigate the functions and pathways of their downstream targets.

Methods: Microarray and stem-loop reverse transcription-polymerase chain reaction were utilized to detect dysregulated miRNA in a rat model. SAM, PAM and clustering analysis were jointly applied to calculate significantly changed miRNA. The targets of miRNA were predicted through web server "microrna." The functions and pathways of those predicted genes were analyzed using databases of Gene Ontology and KEGG by the web server "DAVID."

Results: Fourteen upregulated and six downregulated miRNA were selected as an accurate molecular signature in distinguishing hepatic steatohepatitis from steatosis. Through Gene ontology, 499 and 287 enriched functional categories were found for the target genes of upregulated and downregulated miRNA, including ion homeostasis, protein transport and so on. Through KEGG, 46 and 41 enriched pathways were collected for the target genes of upregulated and downregulated miRNA, including apoptosis, fatty acid metabolism and so on. Analysis of common target genes of all downregulated miRNA revealed potential involvement of ion transport and the membrane structure in steatohepatitis.

Conclusion: We reported the dysregulated miRNA in transition from hepatic steatosis to steatohepatitis and showed potential clinical application in disease differentiation. This study provided data reservoir for miRNA exploration and revealed novel disease-specific Gene Ontology functions and KEGG pathways such as uncoupling-protein-guided membrane change. Our data contributes to further researches on the pathogenesis and treatment of non-alcoholic steatohepatitis.

Introduction

Non-alcoholic fatty liver disease (NAFLD) is defined as a common clinicopathologic condition characterized by lipid deposition in hepatocytes and compromises a wide spectrum of liver damage, including simple steatosis, non-alcoholic steatohepatitis (NASH) and fibrosis.[1] Nowadays, NAFLD has become a major cause of liver-related morbidity and mortality with the incidence of around 20% worldwide[2] and 15% in China.[3] Although the "two-hit hypothesis"[4] has long been recognized as the dominant theory, the pathogenesis of NAFLD is still vague.

MicroRNA (miRNA) belong to a 19–25 nucleotide (nt) non-coding family and are processed from 70- to 100-nt double-stranded hairpin precursors by RNaseIII Dicer and endogenously expressed in the RNA-induced silencing complex in cytoplasm.[5] MiRNA recognize the 3′-untranslated region of target mRNAs with imperfect complementarity to cause translational repression or mRNA cleavage.[6] Since first discovered in *Caenorhabditis elegans* in 1993,[7] miRNA have been found in all multicellular organisms with certain conservations and exert important biological functions.[8] Nowadays, the profile of miRNA is successfully utilized in tumor diagnosis and miRNA-downstream target pairs are actively involved in various diseases and cellular pathways.[9] However, their effects in NAFLD are not widely investigated. Our previous study showed the miRNA profile in different stages of NAFLD,[10] while further study reported unique miRNA in methionine-choline-deficient-diet-induced mice.[11] Nevertheless, the specific miRNA profile responsible for transition from steatosis to non-alcoholic steatohepatitis (NASH) is still vague. Investigation of this transition is of clinical importance, as the risks for cirrhosis and hepatocellular carcinoma are greatly increased in patients suffering from NASH.[12]

© 2011 Journal of Gastroenterology and Hepatology Foundation and Blackwell Publishing Asia Pty Ltd

In this study, we reported the specific miRNA profile of transition from steatosis to steatohepatitis by microarray analysis and stem-loop reverse transcription-polymerase chain reaction (RT-PCR) in a rat model, which might broaden our understanding of NASH progression and become potential targets for therapeutic intervention. Furthermore, the successful differentiation between NASH and steatosis by specific miRNA pattern may serve as a novel diagnostic tool. Finally, bioinformatics methods were used to predict targets of verified miRNA and explore potential downstream Gene Ontology (GO) categories and KEGG pathways of target genes. Those efforts may provide preliminary data for studying certain miRNA-target functions and pathways in the future.

Methods

Experimental animal model, serology and pathology markers

Sprague–Dawley (SD) rats (12 weeks old, 160–170 g) were purchased from the Medical Science Institution of Zhejiang Province (Hangzhou, China) and randomly divided into four groups: S (steatosis, 4 week, $n = 14$), SH (steatohepatitis, 12 weeks, $n = 14$), C4 (control, 4 weeks, $n = 14$) and C12 (control, 12 weeks, $n = 14$). All rats received food and water ad libitum and were maintained on a 12/12-hour light/dark cycle. Control groups were given basic diet while model groups (S, SH) received a fat-rich diet including 80.5% normal diet, 2% cholesterol, 7% lard, 10% yolk powder and 0.5% bile salt.[13] In this formula, 100 g lard contains 110 mg cholesterol and 9.9 g fat, while 100 g yolk powder contains 2 g cholesterol. Rats were killed by femoral exsanguination and serum alanine aminotransferase (ALT), aspartate aminotransferase (AST), triglyceride (TG), total cholesterol (TCh) and hepatic TG were routinely tested. Hepatic index (liver wet weight /bodyweight) were calculated as indicated in the bracket. Hematoxylin–eosin (HE)-stained liver sections were observed and estimated for hepatic steatosis and an Olympus microscope was used to determine inflammation, according to the histological activation index (HAI).[14] This study was approved by the University and Hospital Review Board. All animal studies were conducted according to the regulations for the use and care of experimental animals and the guidelines of the institution.

Microarray and stem-loop RT-PCR

Total RNA retrieved from liver section was purified by *mir*Vana miRNA Isolation Kit (Ambion, Austin, TX, USA) and labeled with Hy3™ fluorescent label with a miRCURY Array Labeling kit (Exiqon, Denmark). The labeled sample was concentrated with an RNeasy Mini Kit (Qiagen, Germany) and further hybridized using a miRCURY Array microarray kit (Exiqon, Denmark). Hybridization signals were scanned with Genepix 4000B (Axon Instruments, Beijing, China) and retrieved images were background subtracted and normalized. Stem-loop RT-PCR was carried out to detect and quantify mature miRNA whose comparative expression levels (SH *versus* S) from microarray results were over 2.0 or below 0.5 by using stem-loop antisense primer mix and AMV transcriptase (TaKaRa, Dalian, China).[15] All primers were purchased from RiboBio (Guangzhou, China) based on miRNA sequences released by Sanger Institute.[16] The relative amount of each miRNA to U6 RNA was calculated using the equation $2^{-\Delta CT}$, where $\Delta C_T = C_{TmiRNA}\text{-}C_{TU6}$.

Bioinformatics analysis of miRNA with significantly differential expression

Raw $-\Delta C_T$ from PCR results were normalized, mean-centered, $\log_2$-transformed and sequentially analyzed by algorithm of SAM (http://www-stat.stanford.edu/~tibs/SAM/), PAM (http://www-stat.stanford.edu/~tibs/PAM/) and hierarchical clustering. SAM calculates a score for each gene as the change of expression relative to the standard deviation of all measurements.[17] In the SAM test, a false discovery rate less to 5% was selected. MiRNA over twofold expression change and Q value < 0.05 were considered significantly altered. Moreover, miRNA signature was determined by PAM, a statistical technique that identifies a subgroup of genes that best characterizes the class of samples.[18] The PAM process was based on training, take-one-out cross validation and testing procedures. The division of samples was done by randomly splitting data into training and test sets. Finally, to visualize numerical changes through graphical representation of the raw $-\Delta C_T$, hierarchical clustering was used to generate both miRNA (from SAM results) and sample (from S and SH) trees based on the algorithm of average linkage and Euclidian distance.[19]

Computational analysis of miRNA downstream targets' functions and pathways

We applied different computational methods to maximally analyze functions and pathways targeted by differentially expressed miRNA. First, an open-access platform for miRNA-target prediction (http://www.microrna.org) was performed to generate predicted targets of significantly altered miRNA. The method is based on a mirSVR scoring system that computes a weighted sum of a number of sequence and context features of the predicted miRNA::mRNA duplex. Generally, a mirSVR score ≤ 0.1 was considered as the cut-off for the positive prediction of miRNA's downstream targets. Thereafter, databases of GO and KEGG pathway were searched for functional annotation and pathway analysis. To exclude those categories just found by chance, the enrichment analysis was further executed using the free access program DAVID,[20] where its significance was measured with Fisher's exact test.

Statistics

Each experiment was performed in triplicate and data were expressed as means ± standard error. The Student's *t*-test for unpaired two groups and one-way ANOVA for three groups were executed by SPSS 11.0 (IBM, New York, USA). The differences were considered statistically significant at $P < 0.05$.

Results

Establishment of NAFLD rat model

The NAFLD rat model was successfully established as confirmed by both serologic and pathologic changes. Comparing with the

© 2011 Journal of Gastroenterology and Hepatology Foundation and Blackwell Publishing Asia Pty Ltd

Table 1 Change of hepatic and serologic markers in steatosis and steatohepatitis

	Group			
	C4	S	C12	SH
Hepatic Index (%)	2.71 ± 0.09	4.56 ± 0.08[a]	3.21 ± 0.13	6.68 ± 0.13[b]
Histological activation index mark	0.68 ± 0.23	0.73 ± 0.16	0.71 ± 0.12	3.85 ± 0.53[c]
Serum triglyceride (mmol/L)	0.52 ± 0.06	0.79 ± 0.04[d]	0.55 ± 0.09	091 ± 0.07[e]
Total cholesterol (mmol/L)	1.65 ± 0.14	2.49 ± 0.36[f]	1.57 ± 0.29	6.20 ± 2.14[g]
Alanine aminotransferase (IU/L)	52.76 ± 6.83	64.75 ± 15.05	59.46 ± 13.08	121.35 ± 27.81[h]
Aspartate aminotransferase (IU/L)	205.13 ± 12.49	214.25 ± 17.51	208.97 ± 16.13	309.51 ± 48.26[i]
Hepatic triglyceride (mmol/L)	1.35 ± 0.07	5.49 ± 0.73[j]	1.49 ± 0.11	5.52 ± 0.96[k]

[a]$P = 0.032$, *vs* C4 group; [b]$P = 0.037$, *vs* S group; [c]$P = 0.012$, *vs* C12 group; [d]$P = 0.041$, *vs* C4 group; [e]$P = 0.023$, *vs* S group; [f]$P = 0.029$, *vs* C4 group; [g]$P = 0.018$, *vs* S group; [h]$P = 0.025$, *vs* C12 group; [i]$P = 0.043$, *vs* C12 group; [j]$P = 0.017$, *vs* C4 group; [k]$P = 0.015$, *vs* C12 group.
Values are expressed as mean ± SE, C4 represents normal 4-week liver group, S represents steatosis group, C12 represents normal 12-week liver group, SH represents steatohepatitis group.

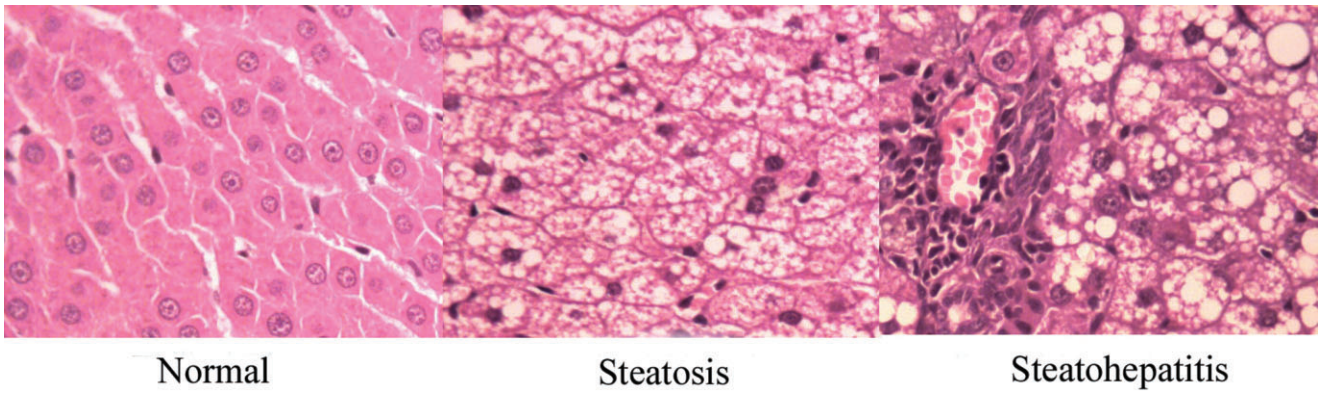

Figure 1 Pathologic presentation of hepatic steatosis and steatohepatitis.

control group, Serum Tch, TG and hepatic index increased dramatically with disease progression while the ALT, AST and histological activation index mark significantly leveled up in NASH stage ($P < 0.05$, Table 1). Simple fatty liver (predominantly macrovesicular) occurred at the 4th week with various degrees of fat deposition as shown by HE staining. At the 12th week, disease progressed to NASH as shown by hepatic lipid accumulation with mild to moderate chronic inflammation of portal and intra-acinar (Fig. 1).

Identification of a unique miRNA profile in differentiating steatohepatitis from steatosis

Initially, miRNA microarray was used to preliminarily screen those differentially expressed mature miRNA. In general, there were 62 miRNA upregulated and 37 miRNA downregulated between steatosis and steatohepatitis as shown in miRNA microarray map (Fig. 2a). Thereafter, a high-throughput stem-loop real-time RT-PCR, which was regarded as the gold standard of RNA quantification, was adapted to confirm the microarray results in randomly selected six samples. Except for eight miRNA (rno-miR-98, rno-miR-16, rno-miR-9, rno-miR-143, rno-miR-298, rno-miR-542-3p, rno-miR-433 and rno-miR-195) within the 0.5–2.0-fold change, the other miRNA showed the same expression patterns as in microarray experiments. The less than 10% discrepancy between these two methods further supports the effectiveness of using microarray for screening dysregulated miRNA.

In order to narrow the scale of dysregulated miRNA, SAM was applied based on raw data of RT-PCR. There were 44 significantly dysregulated miRNA (30 increased and 14 decreased) in the steatohepatitis group when compared with the steatosis group (Table 2). Moreover, the results of hierarchical clustering showed a general distinction between samples of steatohepatitis and steatosis and two major branches in rows (upregulated *versus* downregulated miRNA) were also clearly observed (Fig. 2b). Finally, according to the PAM result, we differentiated samples between steatohepatitis and steatosis by unique miRNA profile composed of 20 miRNA (14 upregulated and 6 downregulated, Fig. 3a). Intriguingly, most of the selected miRNA overlapped with SAM-generated miRNA, further supporting the possibility of using miRNA as potential diagnostic biomarkers. PAM training and cross-validation were conducted using six samples from each group and correctly classified nearly 100% of the samples between the steatohepatitis and steatosis groups (Fig. 3b).

© 2011 Journal of Gastroenterology and Hepatology Foundation and Blackwell Publishing Asia Pty Ltd

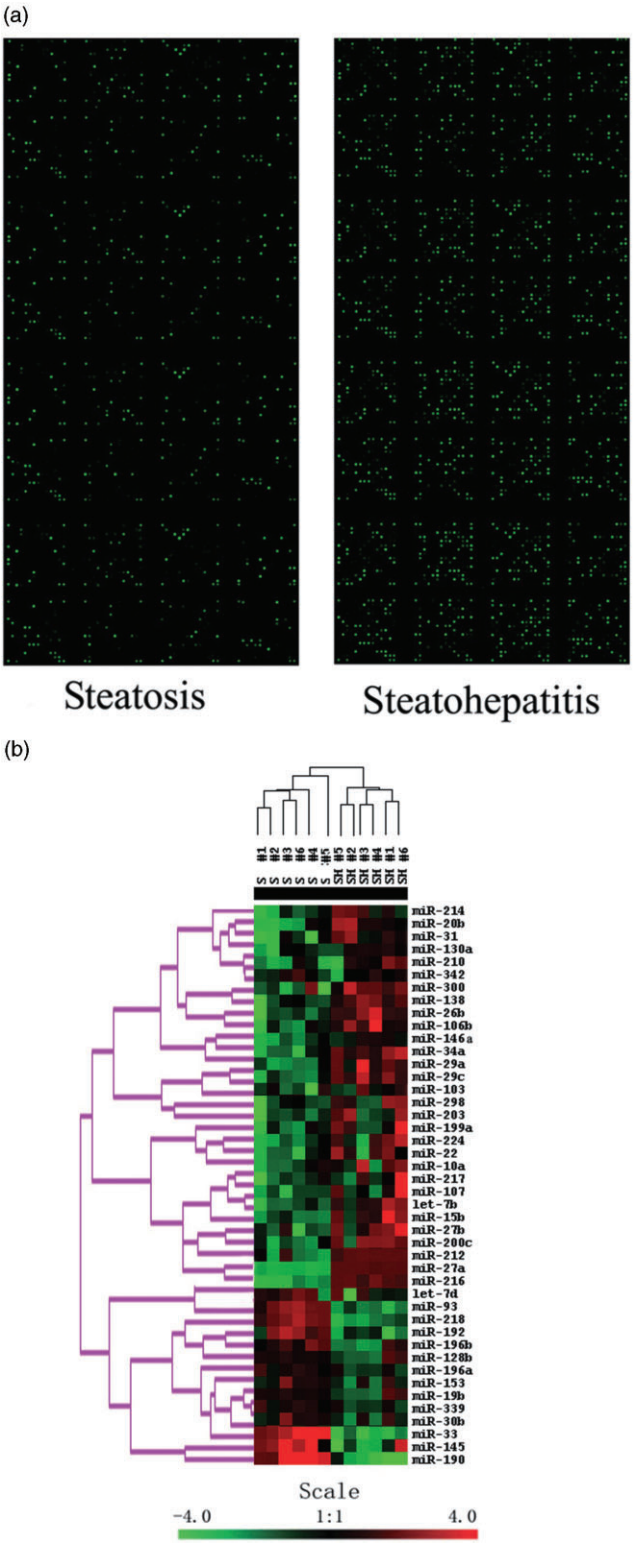

Figure 2 Microarray image and cluster analysis of samples from steatosis and steatohepatitis groups. (a) Microarray image of miRNA. The green signal on the black background indicates the hybridization between tested miRNA and known probes. (b) Dendrogram generated by cluster analysis showed the separation of steatosis from steatohepatitis on the basis of 44 miRNA signature. The clustering was performed on miRNA from SAM results. Red denotes increased expression, green denotes reduced expression and a median expression value equal to 1 is designated by black. Each gene is represented by a single row of colored boxes and each sample is represented by a single column.

Table 2 Significantly dysregulated miRNA between steatohepatitis and steatosis predicted by SAM

miRNA	Fold (Upregulation)	miRNA	Fold (Downregulation)
miR146a	49.5	miR-33	0.04
miR-130a	48.5	miR-19b	0.06
miR-300	33.9	miR-145	0.07
miR-210	28.3	miR-30b	0.07
miR-138	22.4	miR-339	0.09
miR-342	21.9	miR-190	0.10
miR-31	21.5	miR-196b	0.11
miR-29c	18.3	miR-93	0.14
miR-214	18.3	miR-153	0.17
miR-22	16.6	miR-128b	0.18
miR-103	16.0	miR-218	0.18
miR-34a	16.0	miR-192	0.23
miR-106b	15.8	let-7d	0.24
miR-29a	14.4	miR-196a	0.29
let-7b	12.6	ND	ND
miR-212	12.0	ND	ND
miR-216	11.9	ND	ND
miR-203	11.8	ND	ND
miR-10a	11.6	ND	ND
miR-107	11.0	ND	ND
miR-20b-5p	10.7	ND	ND
miR-298	10.6	ND	ND
miR-27b	9.0	ND	ND
miR-15b	8.6	ND	ND
miR-26b	8.0	ND	ND
miR-200c	7.5	ND	ND
miR-224	7.0	ND	ND
miR-217	6.8	ND	ND
miR-199a	6.5	ND	ND
miR-27a	3.4	ND	ND

MiRNA fold change presented here was the mean from six samples of each group, where log2 transformation was performed on raw data. ND, no data.

MiRNA targets' functions and pathways predicted by computer-aided algorithms

The analysis of miRNA-targets' functions and pathways were based on data from the PAM result. We first generated a list of all target genes to those 14 upregulated and six downregulated miRNA. The result showed a total of 3470 and 2173 genes respectively, of which over one-third were expressed in the liver. Thereafter, a functional annotation and over-representation analysis of GO Biological Process (GO BP) terms for those genes were performed using the DAVID program. In this study, a complete list of GO BP terms contained 999 and 681 categories for up and downregulated miRNA. However, as most general GO terms have a tendency to include target genes in a large amount, our analysis

© 2011 Journal of Gastroenterology and Hepatology Foundation and Blackwell Publishing Asia Pty Ltd

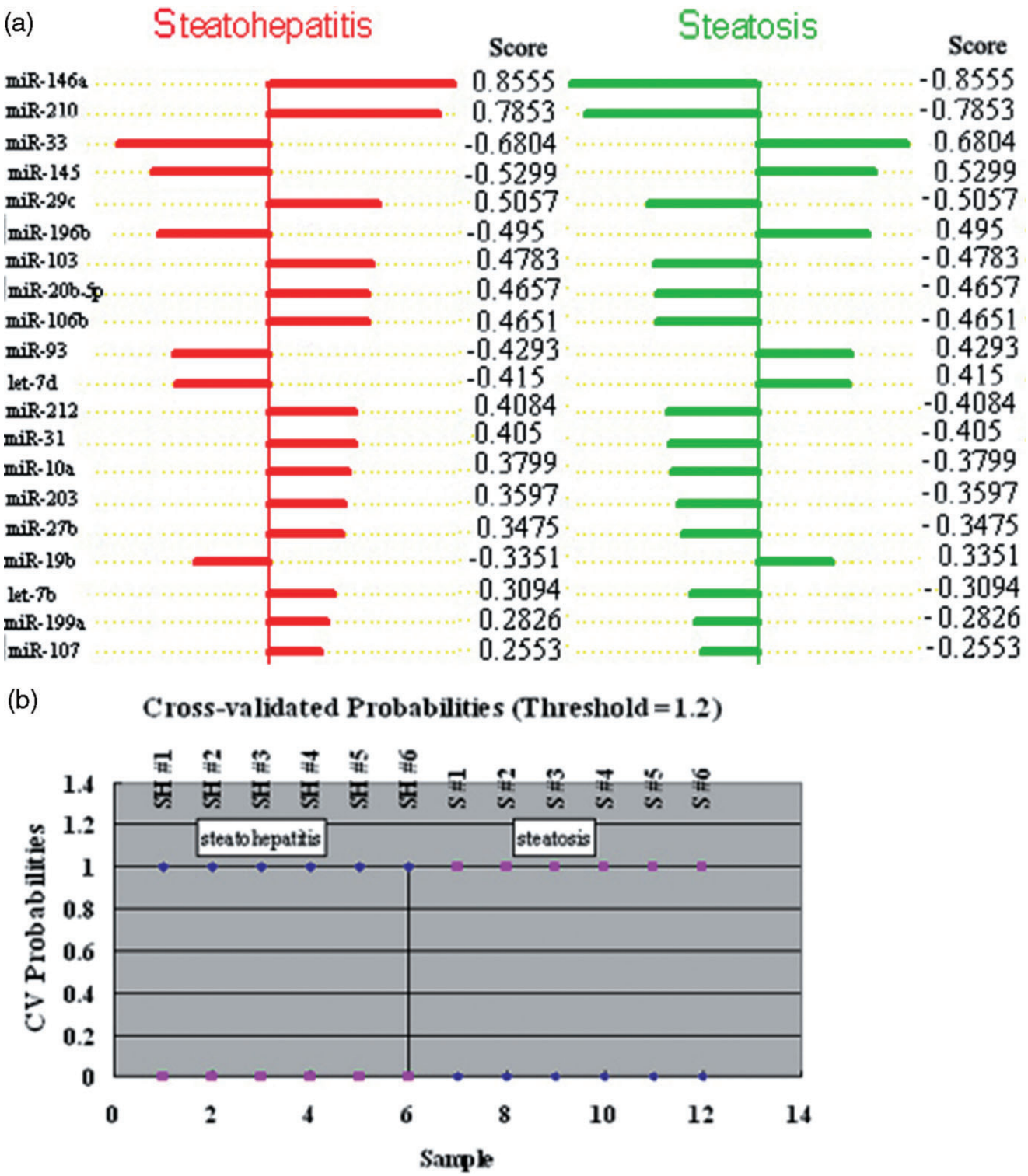

Figure 3 PAM prediction of steatohepatitis from steatosis. (a) PAM results predicted 14 upregulated and six downregulated miRNA in steatohepatitis samples compared to steatosis samples. The miRNA are listed from high to low of PAM score. (b) PAM analysis displayed the graphical representation of the estimated probabilities (0.0–1.0) for the testing samples. Six samples (1–6) from the steatohepatitis group and six samples (7–12) from the steatosis group were nearly 100% correctly classified. ◆, steatohepatitis; ■, steatosis.

© 2011 Journal of Gastroenterology and Hepatology Foundation and Blackwell Publishing Asia Pty Ltd

Table 3 Top 15 categories of up- and downregulated miRNA

Term	Count (%)	*P*-value
Upregulated		
Ion homeostasis	150(4.32)	1.72E-13
Protein transport	187(5.4)	2.5E-12
Intracellular signaling cascade	284(8.2)	4.2E-12
Cellular chemical homeostasis	136(3.9)	2.7E-11
Carboxylic acid metabolic process	176(5.1)	2.1E-10
Regulation of neurological system process	79(2.3)	2.9E-10
Synaptic transmission	87(2.5)	9.8E-10
Regulation of phosphate metabolic process	141(4.1)	2.0E-9
Regulation of phosphorus metabolism process	141(4.1)	2.0E-9
Regulation of transmission of nerve impulse	73(2.1)	2.9E-9
Regulation of synaptic transmission	69(2.0)	5.5E-9
Regulation of membrane potential	65(1.9)	7.7E-9
Positive regulation of cell communication	112(3.2)	1.8E-8
Anion transport	55(1.6)	2.0E-7
Regulation of signal transduction	219(6.3)	2.7E-7
Downregulated		
Protein transport	128(5.9)	6.2E-10
Monovalent inorganic cation transport	74(3.4)	9.4E-8
Ion homeostasis	94(4.3)	1.3E-7
Intracellular signaling cascade	178(8.2)	9.9E-7
Metal ion transport	91(4.2)	5.8E-4
Cellular chemical homeostasis	86(4.0)	1.2E-6
Synaptic transmission	57(2.6)	1.7E-6
Cation transport	105(4.8)	2.5E-6
Regulation of membrane potential	42(1.9)	1.2E-5
Regulation of signal transduction	144(6.6)	1.9E-5
Fatty acid metabolic process	48(2.2)	2.2E-5
Regulation of neurological system process	48(2.2)	2.2E-5
Exocytosis	34(1.6)	2.3E-5
Second-messenger-mediated signaling	44(2.0)	3.1E-5
Regulation of action potential in neuron	23(1.1)	5.0E-5

The categories are listed from high to low *P*-value. Common categories involved in both up and downregulated miRNA are underlined.

Table 4 Top 18 KEGG pathways of up and downregulated miRNA

Term	Count (%)	*P*-value
Upregulated		
Calcium signaling pathway	67(1.9)	6.1E-6
Chemokine signaling pathway	57(1.6)	6.8E-4
Apoptosis	33(1.0)	7.3E-4
Beta-Alanine metabolism	13(0.4)	8.7E-4
Steroid hormone biosynthesis	20(0.6)	9.6E-4
Neuroactive ligand-receptor interaction	80(2.3)	1.1E-3
Neurotrophin signaling pathway	44(1.3)	1.1E-3
Fc gamma R-mediated phagocytosis	33(1.0)	1.4E-3
Lysosome	41(1.2)	1.6E-3
PPAR signaling pathway	27(0.8)	3.5E-3
Cytokine-cytokine receptor interaction	60(1.7)	5.2E-3
Fatty acid metabolism	18(0.5)	5.3E-3
Amyotrophic lateral sclerosis (ALS)	23(0.7)	5.4E-3
Pathways in cancer	90(2.6)	5.5E-3
Cell adhesion molecules (CAM)	47(1.4)	6.1E-3
Adipocytokine signaling pathway	25(0.7)	6.7E-3
Pancreatic cancer	25(0.7)	1.0E-2
Retinol metabolism	22(0.6)	1.2E-2
Downregulated		
Fatty acid metabolism	18(0.8)	1.5E-5
Calcium signaling pathway	44(2.0)	1.5E-4
TGF-beta signaling pathway	24(1.1)	8.7E-4
Neuroactive ligand-receptor interaction	55(2.5)	9.1E-4
PPAR signaling pathway	21(1.0)	9.2E-4
Purine metabolism	36(1.7)	1.3E-3
Chemokine signaling pathway	38(1.7)	2.4E-3
Butanoate metabolism	12(0.6)	3.1E-3
Valine, leucine and isoleucine degradation	14(0.6)	6.8E-3
Long-term potentiation	18(0.8)	7.1E-3
SNARE interactions in vesicular transport	12(0.6)	1.0E-2
Fc gamma R-mediated phagocytosis	21(1.0)	1.3E-2
Maturity onset diabetes of the young	9(0.4)	1.9E-2
Pancreatic cancer	17(0.8)	2.1E-2
MAPK signaling pathway	49(2.3)	2.3E-2
Beta-alanine metabolism	8(0.4)	2.3E-2
Lysosome	25(1.2)	2.4E-2
Steroid hormone biosynthesis	12(0.6)	2.6E-2

The pathways are listed from high to low *P*-value. Common pathways involved in both up and downregulated miRNA are underlined.
MAPK, mitogen-activated protein kinases.

may lose some smaller but more specific genes. For example, the top three categories for those upregulated miRNA are cellular process, regulation of biological quality and transport, which are quite general and not specific to NASH.

To avoid this problem, we performed additional analysis restricted to the lowest level (level 5: GO BP_5) of GO terms. The results showed 499 and 287 more specific functional categories for up- and downregulated miRNA. Table 3 showed the top 15 categories of those up- and downregulated miRNA with eight overlaps, including protein carboxylic acid metabolic process, fatty acid metabolic process, regulation of membrane potential and so on. A similar approach was applied to the enrichment analysis of KEGG pathways for those genes. A total of 46 and 41 pathways were enriched for up- and downregulated miRNA, including apoptosis, fatty acid metabolism, calcium signaling pathway and so on. The top 18 pathways of those up- and downregulated miRNA are listed in Table 4. We cannot predict common targets of 14 upregulated miRNA, but found 12 common targets of six downregulated miRNA (Table 5). As shown in Figure 4a, most targets were related with ion transport and binding as well as the structure and component of membrane, hinting at their potential role in NASH. Besides, the gene-term 2D heat map showed that over half of the gene-term associations have not been reported yet, indicating the novelty of our findings (Fig. 4b). Nevertheless, there were no common pathways for those selected genes.

Discussion

Nowadays, NASH has been considered as a pivotal stage in NAFLD, accounting for the major cause of cryptogenic cirrhosis. A retrospective study showed that 41% and 5.4% of NASH patients progressed to liver fibrosis and end-stage liver diseases.[21] Therefore, it is important to focus on the pathogenesis of NASH. Reports on the expression and effect of miRNA profile in NAFLD

© 2011 Journal of Gastroenterology and Hepatology Foundation and Blackwell Publishing Asia Pty Ltd

Table 5 Common predicted targets of all six downregulated miRNA

Accession	Gene symbol	Full name
NM_022618	Akap6	Akap6 A kinase (PRKA) anchor protein 6
NM_053502	Abcg1	ATP-binding cassette, sub-family G (WHITE), member 1
NM_001024243	Nudt3	Nudix (nucleoside diphosphate linked moiety X)-type motif 3
NM_139192	Scd1	Stearoyl-Coenzyme A desaturase 1
NM_001008880	Scn4b	Sodium channel, voltage-gated, type IV, beta
NM_134363	Slc12a5	Potassium-chloride transporter, member 5
NM_017315	Slc23a1	Nucleobase transporter, member 1
NM_031743	Slc24a2	Sodium/potassium/calcium exchanger, member 2
NM_012758	Syk	Spleen tyrosine kinase
NM_001034083	Snn	Stannin
NM_182667	Myocd	Myocardin
NM_013167	Ucp3	Uncoupling protein 3 (mitochondrial, proton carrier)

are limited.[10,11] Cheung *et al*. reported dysregulated miRNA in human NASH and tabulated their potential targets.[22] Nevertheless, none of these studies has compared specific miRNA responsible for transition from steatosis to steatohepatitis, leaving the blank fulfilled by this study. Moreover, we currently used novel integrative bioinformatics tools to investigate the common gene functional categories and pathways, which is a progress compared to previous studies only predicting common genes of dysregulated miRNA.

In this study microarray was used to screen dysregulated miRNA, followed by stem-loop RT-PCR verification and bioinformatics analysis. As shown in Table 2, the SAM result consisted of 30 increased and 14 decreased miRNA and several listed miRNA were involved in many pivotal pathophysiologic processes. For instance, miR-146a was reported to suppress breast cancer metastasis[23] while miR-31 acted as the overseer of tumor metastasis.[24] In addition, miR-106b showed oncogenic potential in hepatocellular carcinoma,[25] miR-143 targeted KRAS in colorectal tumorigenesis[26] and miR-196b[27] was upregulated in gastric cancer. Some miRNA also participated in hypoxia pathway[28,29] and apoptosis,[30] where these pathways were actively involved in NASH. More importantly, several miRNAs[31,32] were related with adipocyte metabolism and differentiation, a known process in hepatic steatosis. Finally, miR-29c and miR-34a were associated with strain-specific susceptibility to dietary NAFLD,[33] while miR-212-caused leaky gut was found in alcoholic liver disease.[34] However, the effects of those miRNA in transition from steatosis to steatohepatitis were unknown. Therefore, the SAM results provide a reservoir for further studies in steatohepatitis progression.

The PAM analysis made differentiation between steatohepatitis and steatosis become practical. As shown in Figure 3, the differential diagnosis by PAM-selected miRNA had nearly 100% accuracy. However, it is difficult to persuade NAFLD patients to undergo liver biopsy, especially those who have normal ALT levels. Besides, once liver tissue is collected, it is much easier and cheaper to do pathologic evaluation that is a gold standard for NASH diagnosis. In this regard, the PAM result is more useful in scientific research than in clinics. Nevertheless, the emergence of serum miRNA as a non-invasive diagnostic marker provides a novel choice for using miRNA profile in clinical practice.[35] Further research should focus on the successful collection and verification of serum miRNA in the diagnosis of NAFLD.

Using GO and KEGG databases, we found several novel functional categories and biological pathways in NASH. This enrichment analysis made our study different from the latest published article by Alisi *et al*.,[36] where the miRNA profile of different diet-induced NAFLD was expressed and potential down stream proteins were predicted and partially verified. As shown in Table 3, eight miRNA overlap in both top-15 categories of up and down-regulated miRNA. Among them, the regulation of membrane potential is very interesting. As we know, uncoupling protein (UCP) has the capacity in decreasing mitochondrial membrane potential. We previously reported the important role of liver-specific UCP- HDMCP in steatosis formation in NAFLD[37] while in this study we also found that UCP2 was the predicted downstream target of miR-342, miR-298 and miR-214. Those miRNA were all increased in NASH. All these evidences hinted that UCP-guided membrane potential declination might play an important role in the pathogenesis of NASH.

Similarly, we found several important pathways through KEGG (Table 4). Among those overlapped pathways, steroid hormone biosynthesis, PPAR signaling pathway, and fatty acid metabolism were already reported in the pathogenesis of NAFLD while the calcium signaling pathway, lysosome and so on were novel findings. Intriguingly, pancreatic cancer was in the list of pathways of upregulated miRNA as one kind of specific disease, indicating its potential association with NAFLD. In addition, UCP3 belonged to the common genes of those down-regulated miRNA (Table 5) while membrane and transmembrane were in the list of GO categories (Fig. 4a). These data further supported the importance of UCP and membrane integrity in progression to steatohepatitis.

Admittedly, the main limitation of this paper is its nature of description and prediction. We lack concomitant experiments to verify our novel findings. However, as compensation, we used enrichment analysis on the GO category and the KEGG pathway to make full use of retrieved information. In addition, it is still questionable whether the results in rats can be generalized to humans and the difficulty in liver biopsy may hamper their application in clinics. In summary, we provided novel data on specific miRNA profile responsible for transition from steatosis to steatohepatitis while the retrieved specific miRNA signature provided a novel concept for diagnosis. Besides, the miRNA-pair reservoir obtained from this study might broaden our understanding of

© 2011 Journal of Gastroenterology and Hepatology Foundation and Blackwell Publishing Asia Pty Ltd

(a)

1 Cluster(s) Download File

	Annotation Cluster 1	Enrichment Score: 1.92			Count	P_Value	Benjamini
☐	GOTERM_BP_FAT	sodium ion transport	RT		4	5.8E-5	1.9E-2
☐	GOTERM_MF_FAT	alkali metal ion binding	RT		4	4.3E-4	4.0E-2
☐	GOTERM_BP_FAT	monovalent inorganic cation transport	RT		4	1.0E-3	1.6E-1
☐	GOTERM_MF_FAT	sodium ion binding	RT		3	2.6E-3	1.1E-1
☐	GOTERM_BP_FAT	metal ion transport	RT		4	2.7E-3	2.6E-1
☐	GOTERM_MF_FAT	symporter activity	RT		3	3.7E-3	1.1E-1
☐	GOTERM_CC_FAT	integral to membrane	RT		9	4.0E-3	2.2E-1
☐	SP_PIR_KEYWORDS	Symport	RT		3	4.5E-3	2.2E-1
☐	GOTERM_BP_FAT	cation transport	RT		4	4.7E-3	3.3E-1
☐	GOTERM_CC_FAT	intrinsic to membrane	RT		9	4.9E-3	1.5E-1
☐	SP_PIR_KEYWORDS	Sodium	RT		3	5.4E-3	1.4E-1
☐	SP_PIR_KEYWORDS	Sodium transport	RT		3	5.8E-3	1.0E-1
☐	GOTERM_BP_FAT	ion transport	RT		4	1.1E-2	4.6E-1
☐	SP_PIR_KEYWORDS	ion transport	RT		4	1.4E-2	1.8E-1
☐	SP_PIR_KEYWORDS	transport	RT		5	3.0E-2	2.9E-1
☐	UP_SEQ_FEATURE	transmembrane region	RT		7	3.8E-2	8.5E-1
☐	SP_PIR_KEYWORDS	membrane	RT		8	4.4E-2	3.4E-1
☐	SP_PIR_KEYWORDS	transmembrane	RT		7	5.4E-2	3.5E-1
☐	GOTERM_MF_FAT	metal ion binding	RT		6	6.5E-2	8.0E-1
☐	GOTERM_MF_FAT	cation binding	RT		6	6.9E-2	7.4E-1
☐	GOTERM_MF_FAT	ion binding	RT		6	7.3E-2	6.4E-1
☐	UP_SEQ_FEATURE	topological domain:Cytoplasmic	RT		4	3.4E-1	1.0E0
☐	SP_PIR_KEYWORDS	glycoprotein	RT		4	4.4E-1	9.7E-1
☐	UP_SEQ_FEATURE	glycosylation site:N-linked (GlcNAc...)	RT		4	4.8E-1	1.0E0

(b)

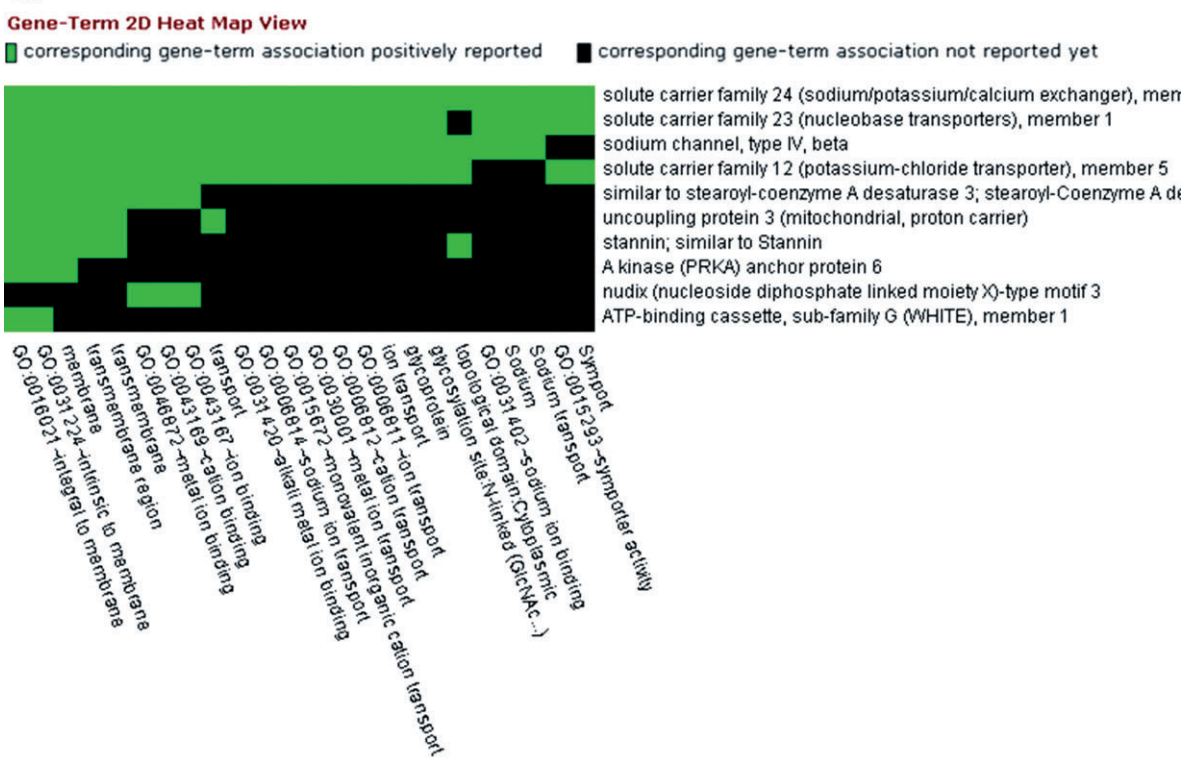

© 2011 Journal of Gastroenterology and Hepatology Foundation and Blackwell Publishing Asia Pty Ltd

Figure 4 Common categories of all downregulated miRNA predicted by PAM. (a) Common GO BP_FAT categories of all downregulated miRNA in differentiating steatohepatitis from steatosis was listed from high to low *P*-value. (b) Gene-term 2-D heat map view shows several unknown gene functions involved in steatohepatitis progression, as presented as black box in the map. Vice versa, the green box indicates known corresponding gene-term association. ■, corresponding gene-term association positively reported; ■, corresponding gene-term association not reported yet.

NASH and become potential targets for therapeutic intervention. Finally, UCP-guided change of membrane potential and integrity needs fierce investigation in the future.

Acknowledgments

This study was sponsored by the 2010 National Natural Science Foundation of China (Project 81000169), the 2010 Excellent Young Investigator Foundation of Health Bureau of Zhejiang Province (Project 2010QNA011), the 2011 Excellent Young Investigator Natural Science Foundation of Zhejiang Province (Project R2110159) and the 2008 National Technology supporting project (2008BAI52B03).

References

1 Angulo P. Nonalcoholic fatty liver disease. *N. Engl. J. Med.* 2002; **346**: 1221–31.
2 Bellentani S, Marino M. Epidemiology and natural history of non-alcoholic fatty liver disease (NAFLD). *Ann. Hepatol.* 2009; **8** (Suppl. 1): S4–8.
3 Fan JG, Farrell GC. Epidemiology of non-alcoholic fatty liver disease in China. *J. Hepatol.* 2009; **50**: 204–10.
4 Day CP, James OF. Steatohepatitis: a tale of two "hits"? *Gastroenterology* 1998; **114**: 842–5.
5 Lau NC, Lim LP, Weinstein EG, Bartel DP. An abundant class of tiny RNAs with probable regulatory roles in Caenorhabditis elegans. *Science* 2001; **294**: 858–62.
6 Ambros V. The functions of animal microRNAs. *Nature* 2004; **431**: 350–5.
7 Lee RC, Feinbaum RL, Ambros V. The C. elegans heterochronic gene lin-4 encodes small RNAs with antisense complementarity to lin-14. *Cell* 1993; **75**: 843–54.
8 Pasquinelli AE, Reinhart BJ, Slack F *et al*. Conservation of the sequence and temporal expression of let-7 heterochronic regulatory RNA. *Nature* 2000; **408**: 86–9.
9 Jay C, Nemunaitis J, Chen P, Fulgham P, Tong AW. miRNA profiling for diagnosis and prognosis of human cancer. *DNA Cell Biol.* 2007; **26**: 293–300.
10 Jin X, Ye YF, Chen SH, Yu CH, Liu J, Li YM. MicroRNA expression pattern in different stages of nonalcoholic fatty liver disease. *Dig. Liver Dis.* 2009; **41**: 289–97.
11 Dolganiuc A, Petrasek J, Kodys K *et al*. MicroRNA expression profile in Lieber-DeCarli diet-induced alcoholic and methionine choline deficient diet-induced nonalcoholic steatohepatitis models in mice. *Alcohol. Clin. Exp. Res.* 2009; **33**: 1704–10.
12 Torres DM, Harrison SA. Diagnosis and therapy of nonalcoholic steatohepatitis. *Gastroenterology* 2008; **134**: 1682–98.
13 Jin X, Yu CH, Lv GC, Li YM. Increased intestinal permeability in pathogenesis and progress of nonalcoholic steatohepatitis in rats. *World J. Gastroenterol.* 2007; **13**: 1732–6.
14 Brunt EM, Janney CG, Di Bisceglie AM, Neuschwander-Tetri BA, Bacon BR. Nonalcoholic steatohepatitis: a proposal for grading and staging the histological lesions. *Am. J. Gastroenterol.* 1999; **94**: 2467–74.
15 Chen C, Ridzon DA, Broomer AJ *et al*. Real-time quantification of microRNAs by stem-loop RT-PCR. *Nucleic Acids Res.* 2005; **33**: e179.
16 Griffiths-Jones S. The microRNA registry. *Nucleic Acids Res.* 2004; **32**: D109–11.
17 Olson NE. The microarray data analysis process: from raw data to biological significance. *NeuroRx* 2006; **3**: 373–83.
18 Tibshirani R, Hastie T, Narasimhan B, Chu G. Diagnosis of multiple cancer types by shrunken centroids of gene expression. *Proc. Natl. Acad. Sci. U S A* 2002; **99**: 6567–72.
19 Eisen MB, Spellman PT, Brown PO, Botstein D. Cluster analysis and display of genome-wide expression patterns. *Proc. Natl. Acad. Sci. U S A* 1998; **95**: 14863–8.
20 Huang da W, Sherman BT, Tan Q *et al*. DAVID Bioinformatics Resources: expanded annotation database and novel algorithms to better extract biology from large gene lists. *Nucleic Acids Res.* 2007; **35**: W169–75.
21 Ekstedt M, Franzen LE, Mathiesen UL *et al*. Long-term follow-up of patients with NAFLD and elevated liver enzymes. *Hepatology* 2006; **44**: 865–73.
22 Cheung O, Puri P, Eicken C *et al*. Nonalcoholic steatohepatitis is associated with altered hepatic MicroRNA expression. *Hepatology* 2008; **48**: 1810–20.
23 Hurst DR, Edmonds MD, Scott GK, Benz CC, Vaidya KS, Welch DR. Breast cancer metastasis suppressor 1 up-regulates miR-146, which suppresses breast cancer metastasis. *Cancer Res.* 2009; **69**: 1279–83.
24 Valastyan S, Weinberg RA. miR-31: a crucial overseer of tumor metastasis and other emerging roles. *Cell Cycle* 2010; **9**: 2124–9.
25 Li Y, Tan W, Neo TW *et al*. Role of the miR-106b-25 microRNA cluster in hepatocellular carcinoma. *Cancer Sci.* 2009; **100**: 1234–42.
26 Chen X, Guo X, Zhang H *et al*. Role of miR-143 targeting KRAS in colorectal tumorigenesis. *Oncogene* 2009; **28**: 1385–92.
27 Tsai KW, Hu LY, Wu CW *et al*. Epigenetic regulation of miR-196b expression in gastric cancer. *Genes Chromosomes Cancer* 2010; **49**: 969–80.
28 Rane S, He M, Sayed D *et al*. Downregulation of miR-199a derepresses hypoxia-inducible factor-1alpha and Sirtuin 1 and recapitulates hypoxia preconditioning in cardiac myocytes. *Circ. Res.* 2009; **104**: 879–86.
29 Huang X, Le QT, Giaccia AJ. MiR-210–micromanager of the hypoxia pathway. *Trends Mol. Med.* 2010; **16**: 230–7.
30 Guo CJ, Pan Q, Li DG, Sun H, Liu BW. miR-15b and miR-16 are implicated in activation of the rat hepatic stellate cell: an essential role for apoptosis. *J. Hepatol.* 2009; **50**: 766–78.
31 Karbiener M, Fischer C, Nowitsch S *et al*. microRNA miR-27b impairs human adipocyte differentiation and targets PPARgamma. *Biochem. Biophys. Res. Commun.* 2009; **390**: 247–51.
32 Wilfred BR, Wang WX, Nelson PT. Energizing miRNA research: a review of the role of miRNA in lipid metabolism, with a prediction that miR-103/107 regulates human metabolic pathways. *Mol. Genet. Metab.* 2007; **91**: 209–17.
33 Pogribny IP, Starlard-Davenport A, Tryndyak VP *et al*. Difference in expression of hepatic microRNAs miR-29c, miR-34a, miR-155, and miR-200b is associated with strain-specific susceptibility to dietary nonalcoholic steatohepatitis in mice. *Lab. Invest.* 2010; **90**: 1437–46.

© 2011 Journal of Gastroenterology and Hepatology Foundation and Blackwell Publishing Asia Pty Ltd

34 Tang Y, Banan A, Forsyth CB *et al*. Effect of alcohol on miR-212 expression in intestinal epithelial cells and its potential role in alcoholic liver disease. *Alcohol. Clin. Exp. Res.* 2008; **32**: 355–64.
35 Lawrie CH, Gal S, Dunlop HM *et al*. Detection of elevated levels of tumour-associated microRNAs in serum of patients with diffuse large B-cell lymphoma. *Br. J. Haematol.* 2008; **141**: 672–5.
36 Alisi A, Da Sacco L, Bruscalupi G *et al*. Mirnome analysis reveals novel molecular determinants in the pathogenesis of diet-induced nonalcoholic fatty liver disease. *Lab. Invest.* 2011; **91**: 283–93.
37 Jin X, Yang YD, Chen K *et al*. HDMCP uncouples yeast mitochondrial respiration and alleviates steatosis in L02 and hepG2 cells by decreasing ATP and H2O2 levels: a novel mechanism for NAFLD. *J. Hepatol.* 2009; **50**: 1019–28.

© 2011 Journal of Gastroenterology and Hepatology Foundation and Blackwell Publishing Asia Pty Ltd